IEEE Photonics Journal
An IEEE Photonics Society Publication

Open Access

Effect of Carrier Localization and Shockley-Read-Hall Recombination on the Spatial Distribution of Electroluminescence in InGaN LEDs

Volume 10, Number 6, December 2018

Zhangbao Peng
Yijun Lu
Yulin Gao
Guolong Chen
Jianfei Zheng
Ziquan Guo
Yue Lin
Zhong Chen

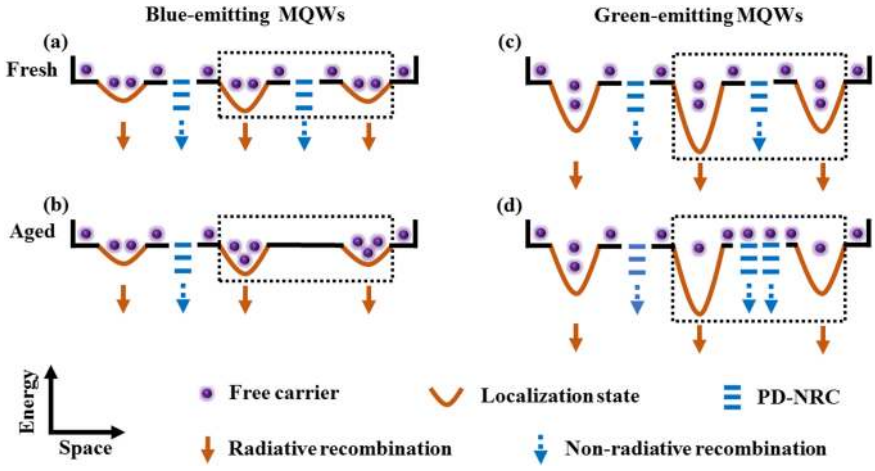

DOI: 10.1109/JPHOT.2018.2880319
1943-0655 © 2018 IEEE

Effect of Carrier Localization and Shockley-Read-Hall Recombination on the Spatial Distribution of Electroluminescence in InGaN LEDs

Zhangbao Peng,[1] Yijun Lu,[1] Yulin Gao,[1] Guolong Chen,[1] Jianfei Zheng,[2] Ziquan Guo,[1] Yue Lin,[1] and Zhong Chen [1]

[1]Department of Electronic Science, Fujian Engineering Research Center for Solid State Lighting, Collaborative Innovation Center for Optoelectronic Semiconductors and Efficient Devices, Xiamen University, Xiamen 361005, China
[2]Xiamen Dacol Photoelectronics Technology Co., Ltd., Xiamen 361100, China

DOI:10.1109/JPHOT.2018.2880319

Manuscript received September 29, 2018; revised October 28, 2018; accepted November 5, 2018. Date of publication November 9, 2018; date of current version November 22, 2018. This work was supported in part by the National Natural Science Foundation of China under Grants 61504112, 11604285, and 51605404, in part by the Natural Science Foundation of Fujian Province under Grant 2018J01103, in part by the Science and Technology Planning Project of Fujian Province under Grant 2018H6022, in part by the Technological Innovation Project of Economic and Information Commission of Fujian Province, and in part by the Strait Postdoctoral Foundation of Fujian Province. Corresponding authors: Yue Lin; Zhong Chen (e-mail: yue.lin@xmu.edu.cn; chenz@xmu.edu.cn).

Abstract: We investigate divergent behaviors in the emission of blue and green light-emitting diodes (LEDs) when they are subjected to the current-stress aging. Microscopic hyperspectral imaging is introduced to measure spatially resolved mappings of the peak intensity, the peak energy, and the full width at half maximum. Also, plots of external quantum efficiency versus injection current are measured to determine the extent of the Shockley-Read-Hall (SRH) nonradiative recombination rate based on the two-level model. As a result, a phenomenological model is proposed to account for the competitive mechanism between the carrier localization and the SRH recombination. In the blue LED case, the increase in the radiative recombination within localization states cancels the SRH nonradiative recombination within point defects. While in the green LED case, the enhancement of SRH recombination and the remission of carrier localization jointly kill the radiative recombination.

Index Terms: Light-emitting diodes, microscopic hyperspectral imaging, carrier localization, Shockley-Read-Hall recombination.

1. Introduction

Studies on the efficiency vibration of light-emitting diodes (LEDs) subjected to aging processes shed light into research on physical mechanisms of the carrier recombination in the active layer [1]–[3]. Though behaviors during the aging may differ drastically among samples, they at least share a common phenomenon that all kinds of stresses, e.g., current and/or temperature, lead to fierce vibrations of the efficiency within an initial short period after the aging, and those of the efficiency gradually become milder thereafter [4], [5]. It literally indicates that the crystalline structure of LED devices remains unstable at the very beginning, but will reach a quasi-steady state after a period of interaction with successive flows of high-energy electrons. However, when performing optical

measurements during the aging, previous works studied the chip under investigation in an integrated manner, in which the light emission of the whole chip is collected via an integrating sphere. It therefore has abandoned the information of possible spatial inhomogeneity along the chip surface [6]. In general, spatially resolved emission spectra can be obtained by a spectroscopy integrated with a transmission electron microscopy [7], scanning near-field microscopy [8], confocal microscopy [9], and atomic force microscopy [10]. Through these photo- and cathode-techniques, crystal imperfections, indium clusters, and polarization fields have been considered being associated with emission processes. In our previous research on the spatially resolved photoluminescence (PL) and electroluminescence (EL) of blue LED chips, it is found that the surficial luminance can be so un-uniform that, except for the intensity vibration, the peak energy and the full width at half maximum (FWHM) of EL and PL spectra collected from each point divert from each other [11], [12]. Mappings of these three spatially resolved parameters of EL and PL spectra jointly provide insight into the evolution of the interplay between carriers and lattices. As lattices are modified during the interaction with plenty of energetic electrons, the inhomogeneity or patterns of such spatially resolved mappings probably change during aging tests. Besides, compositional fluctuations can be enhanced by the increasing indium composition, accompanying with the deterioration of the crystal quality due to the large lattice immiscibility of InN and GaN in InGaN/GaN active layers [13]. The study on these evolutions therefore can uncover some physical processes that have not yet been found by previous research.

In this work, for two types of LEDs—blue ones with lower indium contents and green ones with higher, we investigate spatially resolved EL characteristics, which are carried out via a microscopic hyperspectral imaging (MHI) system [14]. All spatially resolved mappings of the peak intensity, the peak energy and the FWHM for blue and green LEDs are obtained before and after the aging. Also measured are fitting parameters of the external quantum efficiency as a function of injection current (EQE $- I_f$) by the two-level model, which is to estimate the capability of Shockley-Read-Hall (SRH) non-radiative recombination centers (NRCs) [11], [12]. Based on above analyses, a phenomenological model concerning the carrier localization effect [15] and the SRH recombination is presented to describe possible mechanisms of the carrier recombination in In-rich LEDs.

2. Experimental Details

Two types of LED samples employed in this work are grown on *c*-plane sapphire substrates via metal-organic chemical vapor deposition. Nominal indium mole fractions in InGaN/GaN multiple quantum wells (MQWs) are ∼20% for the blue LED and ∼35% for the green LED, and corresponding integrated EL emissions of samples are located at ∼454 nm (∼2.73 eV) and ∼537 nm (∼2.31 eV), respectively. Except for the difference of indium contents, all samples are similar, and fabrication processes of chips (1 mm × 1 mm) are described in detail elsewhere [12], [16]. Aging tests are carried out by a high-power LEDs aging system (ZWL-190, Zhongwei Photoelectricity Inc., China), and the stress current is set at $I_f = 850$ mA ($J_f = 85$ A/cm^2). During measurements, samples are driven by a current source (Keithley 2400, Keithley Inc., USA), and the heat-sink temperature is controlled to 25 °C by using a TEC temperature controller (LED-850, Instrument Systems Corp., Germany). Spatially resolved mappings are captured by a MHI system, which features a microscope (MJ51, Mingmei Inc., China), and a portable hyperspectral camera (GaiaField-F-V10, Shuanglihepu Inc., China). A detailed description of MHI system can be found in our pervious report [17]. Note that all EL mappings are captured at a series of I_f, ranging from 0.5 mA to 80 mA ($J_f = 0.05 - 8$ A/cm^2) at room temperature.

3. Results and Discussion

3.1 Description of Experimental Results

To investigate possible aging mechanisms related to In-rich InGaN MQWs at small injection currents, we evaluate characteristics of EL spectra extracted from spatially resolved mappings. To avoid the

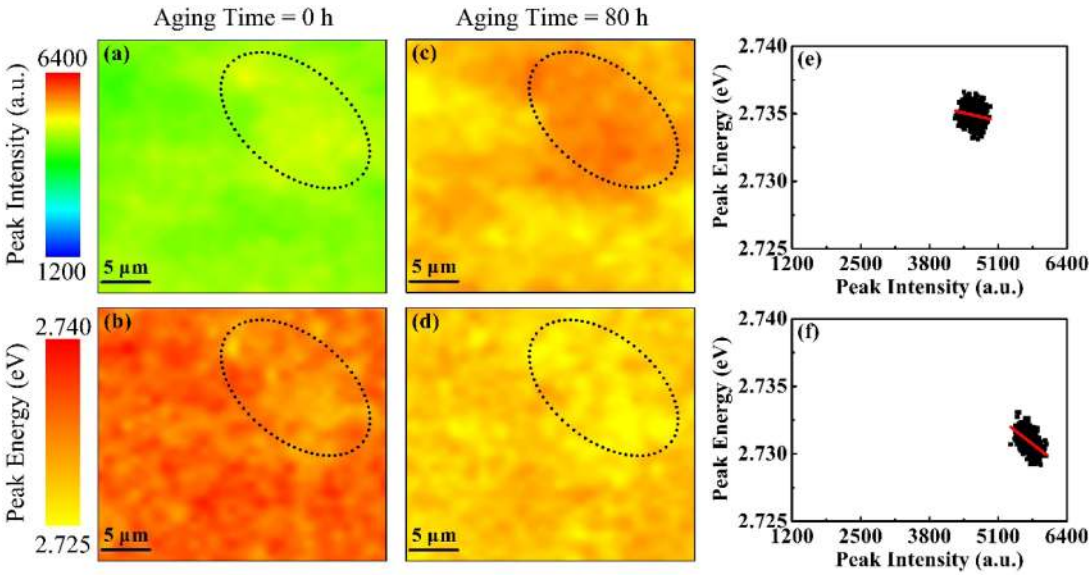

Fig. 1. Mappings of the peak intensity at 0 h (a) and 80 h (c), and the peak energy at 0 h (b) and 80 h (d) for the blue LED measured at 1 mA. Relationship between the peak intensity and the peak energy at 0 h (e) and 80 h (f). Dotted circles in MHI mappings indicate areas with high peak intensity and low peak energy. Solid red lines in *E-I* clouds imply the anti-correlation between the peak intensity and the peak energy.

influence of electrodes and bonding leads, for each sample, six patches of area on the surface are selected for the investigation. Among them, similar results are observed and MHI mappings of a typical one (30 μm $\times$ 30 μm) are described in detail below. Each mapping, detected at a series of injection currents (0.5–80 mA), consists of 3600 (60 $\times$ 60) pixels.

As illustrated in Fig. 1, all mappings of the peak intensity and the peak energy for the blue LED before and after the 80-hour aging are inhomogeneous. In Fig. 1(a), a region with intensity slightly higher than surrounding areas lies in the up-right. This region is roughly associated with the low-energy region, as shown in Fig. 1(b). However, little anti-correlation can be observed in the plot of peak energy verse the peak intensity (*E-I* cloud) [Fig. 1(e)]. After the 80-hour aging, the peak intensity increases, but retains the inhomogeneity [Fig. 1(c)]. The peak energy decreases (red-shift in the peak wavelength), also preserves the fluctuation [Fig. 1(d)]. As plotted in Fig. 1(f), the *E-I* cloud evolves into an eclipse with an inclined long axis, which reveals a strong anti-correlation after the aging. We can also observe mappings of the peak intensity and the peak energy, which illustrate that the high brightness region and low-energy region precisely coincides. It reveals that regions with lower band-gap are populated with carriers, resulting in stronger band-edge recombination. Similar phenomena are reported in our previous work [11], in which we suggest that the carrier localization effect induced by compositional fluctuations of the InGaN alloy or thickness fluctuations of InGaN well layers, is able to prevent free carriers from diffusing into NRCs and thus enhance the radiative recombination. In this work, by comparison between the fresh and aged sample, we further prove that such anti-correlation effect can be intensified under the constant high injection current, leading to the increase in the peak intensity and the red-shift in the peak energy.

However, we do not observe such anti-correlation between the peak intensity and the peak energy for green LEDs, as shown in Fig. 2. All mappings before and after the aging [Fig. 2(a)–(d)] illustrate weak inhomogeneity, compared with its blue counterparts. Instead of the anti-correlation, the *E-I* cloud of the fresh sample exhibits some degree of positive correlation between the peak intensity and the peak energy [Fig. 2(e)], i.e., regions with higher brightness are accompanied with higher peak energy. After the aging, the positive correlation fades as the intensity becomes uniform [Fig. 2(f)]. As one type of In-rich LED devices, more indium incorporated in the green LED gives rise

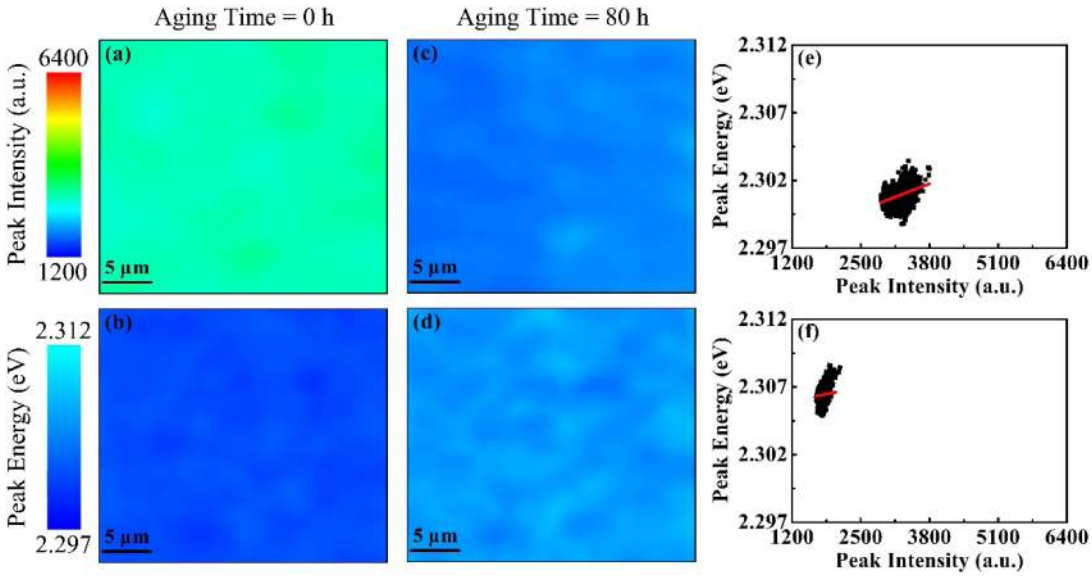

Fig. 2. Mappings of the peak intensity at 0 h (a) and 80 h (c), and the peak energy at 0 h (b) and 80 h (d) for the green LED measured at 1 mA. Relationship between the peak intensity and the peak energy at 0 h (e) and 80 h (f). Solid red lines in *E-I* clouds imply the positive correlation between the peak intensity and the peak energy.

to numerous crystal imperfections and thus enhances the SRH non-radiative recombination [18]. In literature [19], extended defects such as dislocations are identified as a mostly undesirable SRH NRCs when they are susceptible to high inject current because of the rise in the carrier diffusion length as well as its mobility on this occasion. Therefore, point defects (PDs), a nanoscopic crystal imperfection, including vacancies, interstitials, and impurities, are mainly responsible for the severe SRH non-radiative recombination in view of the small injection current of 1 mA in this work, especially for the aged sample.

Mappings of the linewidth, measured as FWHM, are plotted in Fig. 3(a)–(d), which reveal the fact that opposite changes occur in the blue LED and the green LED. Namely, after the aging, the FWHM tends to be broadened for the former, while narrowed for the latter. Normalized EL spectra of two types of LED devices are exhibited in Fig. 3(e)–(f), and original EL spectra are illustrated in insets of them. Both for blue and green LEDs, only a little change appears in high-energy wings of spectra after the aging. However, low-energy wing changes conspicuously as broadening and narrowing are observed for blue and green spectra, respectively. In the meantime, aged spectra exhibit slight shifts in the peak energy, which is in consistent with the observation of MHI mappings of the peak energy described above, accompanied by a red-shift for the blue LED and a blue-shift for the green one. Previous works [20], [21] pointed out that the FWHM is associated with nanometer-scale potential fluctuations, which function as the localization centers while altering the spectrum in the low-energy side. Therefore, we can conjecture that such opposite changes of FWHMs are attributed to the enhancement of carrier localization effect in the blue LED and to the remission of it for the green one.

To further determine the evolution of the SRH non-radiative recombination, we introduce the two-level model, which is an alternative way of evaluating the rising segment of the EQE $- I_f$ curve and can be expressed as [12], [16]:

$$\eta_{\mathrm{EQE}} = \frac{C[1 - (\alpha + \beta)/I_f + \sqrt{4\alpha/I_f + (1 - (\alpha + \beta)/I_f)^2}}{2}, \tag{1}$$

where η_{EQE} denotes the external quantum efficiency, which is calculated from all pixels in the MHI mapping; C is a constant, depending on the light extraction rate of LED devices; α and β are

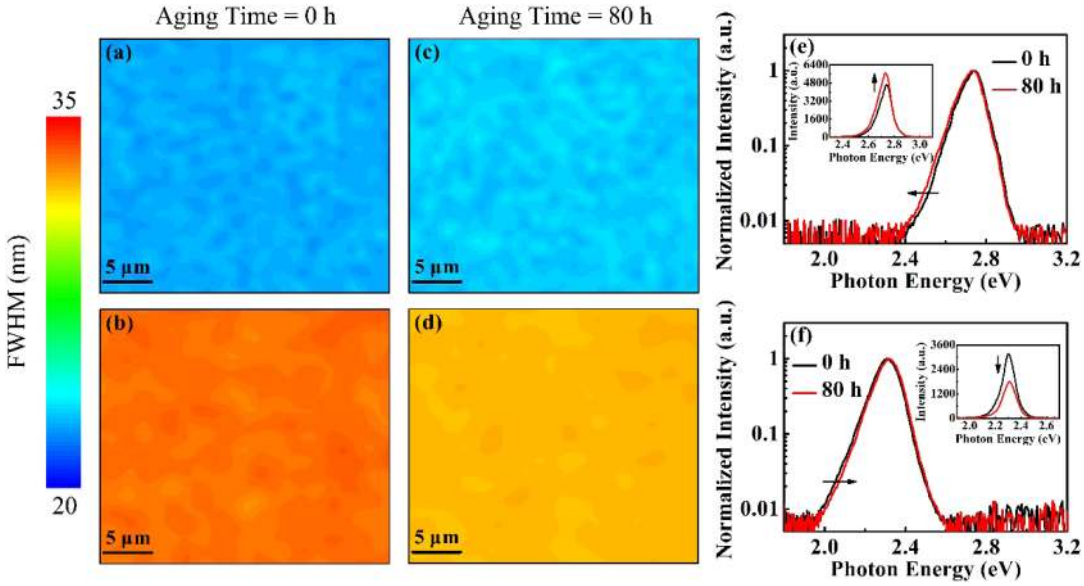

Fig. 3. Mappings of the FWHM at 0 h (a) and 80 h (c) for the blue LED, and 0 h (b) and 80 h (d) for the green LED measured at 1 mA. Normalized EL spectra (in logarithmic scale), captured from all pixels in the representative square area, of the blue LED (e) and the green LED (f). Insets: Original EL spectra (in linear scale).

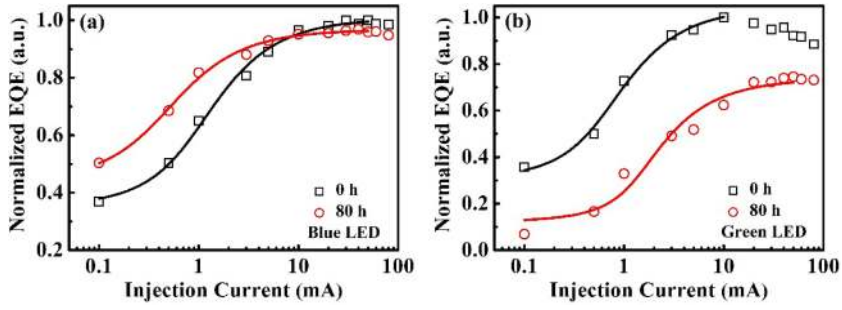

Fig. 4. Plots of normalized EQE vs. I_f for (a) the blue LED and (b) the green LED. All EQEs are normalized to the peak EQE at 0 h and solid lines are the fitting results based on the two-level model.

parameters related to the recombination rate between the interband radiative and non-radiative recombination mainly via PDs. It is worth noting that we focus on the ratio of β to α, namely, $\zeta = \beta/\alpha$, which is regarded as an indicator of the ability of capturing carriers for all PDs in the active layer. Fitting curves via the two-level model are plotted in Fig. 4 and all fitting parameters are listed in Table 1. For the blue LED [Fig. 4(a)], the value of ζ exhibits a slight decrease from 1.83 to 1.17, indicating that the SRH recombination is alleviated in the aged sample. On the contrary, the value of ζ shows a remarkable increase from 2.41 to 5.05, implying that the SRH recombination is greatly reinforced in the aged green LED [Fig. 4(b)]. It is reasonable to deduce the fact that distinct modifications of PDs can account for different behaviors of the SRH recombination in both LED MQWs. Contrary to blue LED MQWs, numerous PDs are possibly created by the high-current stress in green LED ones.

3.2 Phenomenological Model

Experimental results presented above uncover a fact that the correlation between the carrier localization effect and the SRH recombination is widely divergent during the aging. The discrepancy

TABLE 1
Fitting Parameters Used in the Two-Level Model of the Blue LED and the Green LED

Sample	Blue LED		Green LED	
	0 h	80 h	0 h	80 h
C	1.01	0.97	1.04	0.74
α (mA)	0.30	0.18	0.17	0.21
β (mA)	0.55	0.21	0.41	1.06
$\zeta = \beta/\alpha$	1.83	1.17	2.41	5.05

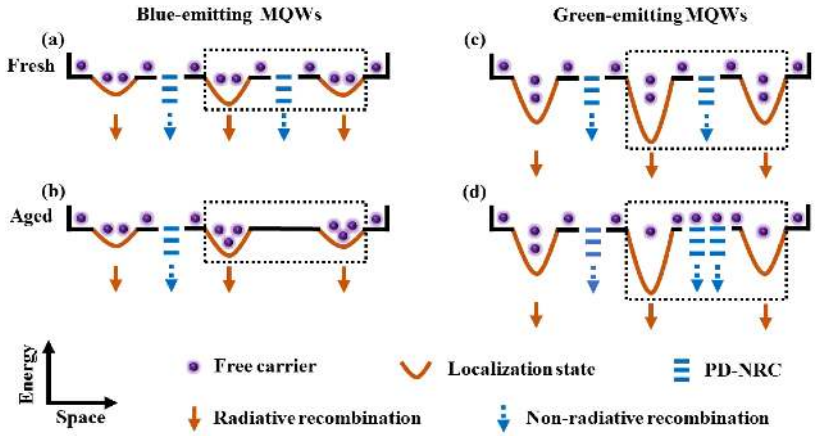

Fig. 5. The schematic of carrier recombination evolution of blue-emitting MQWs and green-emitting MQWs in the case of (a) and (c) fresh, (b) and (d) aged. Evolutionary processes are mainly depicted in dotted frames.

in aging behaviors of the blue LED and the green LED possibly stems from the difference of indium contents. The carrier localization effect caused by indium fluctuations in the active region can enhance the radiative recombination by trapping carriers into localization centers [22], [23]. Nevertheless, NRCs mainly introduced by PDs can assimilate free carriers escaped from localization centers and accelerate the SRH non-radiative recombination rate [24]. Therefore, the net influence on the peak intensity is the result of the competition between the carrier localization effect and the SRH recombination. In general, in indium-dilute devices, the former effect dominates, and the increasing indium content brings the latter into play.

A phenomenological model is proposed to explain competitive mechanisms at small injection current in detail, as depicted in Fig. 5. Three types of carrier recombination processes, namely the band-edge radiative recombination, the localized recombination, and the SRH recombination, occur simultaneously while they compete with each other as carriers are injected into active regions. The first type, as its name suggested, takes place in the band-edge, ending up emitting a photon with energy equal to the band-gap. The second type also occurs in a special band-edge region, where the energy is slightly lower than surrounding areas, namely the localization center, which is located at sites of In-rich clusters and quantum-dots-like structures [25]. In general, recombination in the localization center is also mostly radiative, but emits a photon with slight lower energy than in the first type. The third type, however, being non-radiative, takes part in SRH NRCs, which mostly consist of PDs. This miniature crystal imperfection is quasi-stable, such that can be modified under the sustaining impact of energetic electrons, resembling the annealing effect, which can reduce effective density of PDs [26]. The modification of aged blue-emitting MQWs [Fig. 5(b)] manifests that PDs are partly removed by the high injection current. However, in green-emitting MQWs,

localization states are deeper than those in blue-emitting ones, because severe phase separation and indium segregation are usually formed in the indium abundant region [27]. Meanwhile, the high indium content can result in the grievous mismatched strain at InGaN/GaN interfaces and facilitate the proliferation of PDs [28]. While lattices are being subjected to successive flows of high-energy electrons, the density of PDs is elevated [Fig. 5(d)]. During the high current aging, high-energy electrons may recombine non-radiatively at original PDs and then release extra energies to motivate the creation of new PDs or to enable original PDs to move [29]. Detailed mechanisms related to the generation of PDs principally include the diffusion of Mg atoms from the p-type layer [30], the formation of nitrogen and gallium vacancies [31], the migration of indium atoms [32], and the intrusion of ambient impurities such as carbon [33].

In the case of blue-emitting MQWs, as sketched in Fig. 5(a)–(b), decreasing PDs caused by the annealing effect mitigate the portion of SRH non-radiative recombination. The reduction in PDs has been revealed by the fitting parameter of the two-level model [Fig. 4(a)]. Therefore, after the aging, more carriers are recombining at the band-edge and/or localization centers because of the improvement of the carrier mobility and the diffusion length [19], [34], [35]. The enhancement of localization effect has also been indicated by the anti-correlation between the peak intensity and the peak energy [Fig. 1], as well as the expansion of low-energy wing of the aged EL spectrum [Fig. 3(e)]. Free carriers tend to be recombined radiatively in the lower energy region, leading to the higher intensity at lower energy sites.

In the case of green-emitting MQWs, the trend is quite opposite, as sketched in Fig. 5(c)–(d). In fact, due to the introduction of additional PDs caused by the high-current aging, the shorter carrier diffusion length is expected to increase the probability of non-radiative recombination, which suppresses the radiative one in band-edge levels and localization states [34], [35]. The increment in PDs has been estimated by the fitting parameter of the two-level model [Fig. 4(b)]. Thus, the peak intensity decreases rapidly after the aging, especially at the low injection region where carriers are susceptible to PDs. The diminishing localization effect also can be evidenced in the shrinking low-energy wing of the aged EL spectrum [Fig. 3(f)].

4. Conclusion

Two types of In-rich devices are used to investigate possible mechanisms of the carrier transmission and recombination in InGaN/GaN MQWs. During the aging, the carrier localization effect is enhanced in the blue LED while weakened in the green one. Meanwhile, the SRH recombination is estimated to be distinctly different for two types of In-rich LEDs after the aging. Based on results of spatially resolved mappings of the peak intensity, the peak energy and the FWHM, we propose a phenomenological model in the carrier transfer between the effect of carrier localization and the SRH recombination. For blue-emitting MQWs, injected carriers tend to participate the radiative recombination in localization centers, rather than interact with neighboring SRH NRCs mainly created by PDs. This positive effect leads to the increase in the peak intensity and the decrease in the peak energy, as well as the broadening of the FWHM. However, for green-emitting MQWs, weakened localization potentials can no longer hold as many carriers as they did before the aging, thus injected carriers are susceptible to PDs, of which the density is even elevated after the aging. Consequently, less populated band-edge recombination results in the decrease in the peak intensity and the increase in the peak energy, as well as the shrinking of the FWHM.

References

[1] B. Sun, X. P. Jiang, K. C. Yung, J. J. Fan, and M. G. Pecht, "A review of prognostic techniques for high-power white LEDs," *IEEE Trans. Power Electron.*, vol. 32, no. 8, pp. 6338–6362, Aug. 2017.

[2] A. Vaskuri *et al.*, "Relationships between junction temperature, electroluminescence spectrum and ageing of light-emitting diodes," *Metrologia*, vol. 55, no. 2, pp. S86–S95, Mar. 2018.

[3] X. H. Qu, H. Wang, X. Q. Zhang, F. Blaabjerg, and H. S. H. Chung, "A lifetime prediction method for LEDs considering real mission profiles," *IEEE Trans. Power Electron.*, vol. 32, no. 11, pp. 8718–8727, Nov. 2017.

[4] L. Canale, P. Dupuis, S. Leng, and G. Zissis, "Study of high-brightness LED samples aged under stress temperature conditions: Electrical characterizations and signature evolution analysis," *IEEE Trans. Ind. Appl.*, vol. 52, no. 1, pp. 502–510, Jan. 2016.

[5] D. Monti *et al.*, "Defect-related degradation of AlGaN-based UV-B LEDs," *IEEE Trans. Electron Devices*, vol. 64, no. 1, pp. 200–205, Jan. 2017.

[6] M. Buffolo, C. D. Santi, M. Meneghini, D. Rigon, G. Meneghesso, and E. Zanoni, "Long-term degradation mechanisms of mid-power LEDs for lighting applications," *Microelectron. Reliab.*, vol. 55, no. 9–10, pp. 1754–1758, Jul. 2015.

[7] P. F. Zhu, W. Wang, H. Y. Zhu, P. Vargas, and A. Bont, "Optical properties of Eu^{3+}-doped Y_2O_3 nanotubes and nanosheets synthesized by hydrothermal method," *IEEE Photon. J.*, vol. 10, no. 1, Feb. 2018, Art. no. 4500210.

[8] R. Ivanov, S. Marcinkevičius, T. K. Uždavinys, L. Y. Kuritzky, S. Nakamura, and J. S. Speck, "Scanning near-field microscopy of carrier lifetimes in m-plane InGaN quantum wells," *Appl. Phys. Lett.*, vol. 110, no. 3, Jan. 2017, Art. no. 031109.

[9] Y. C. Leem and S. Y. Yim, "Microscopic observation of low efficiency in green light-emitting diodes," *ACS Photon.*, vol. 5, no. 3, pp. 1129–1136, Jan. 2018.

[10] F. C. P. Massabuau *et al.*, "Morphological, structural, and emission characterization of trench defects in InGaN/GaN quantum well structures," *Appl. Phys. Lett.*, vol. 101, no. 21, Nov. 2012, Art. no. 212107.

[11] Y. Lin *et al.*, "Spatially resolved study of quantum efficiency droop in InGaN light-emitting diodes," *Appl. Phys. Lett.*, vol. 101, no. 25, Dec. 2012, Art. no. 252103.

[12] Y. Lin *et al.*, "Interplay of point defects, extended defects, and carrier localization in the efficiency droop of InGaN quantum wells light-emitting diodes investigated using spatially resolved electroluminescence and photoluminescence," *J. Appl. Phys.*, vol. 115, no. 2, Jan. 2014, Art. no. 023103.

[13] G. P. Dimitrakopulos *et al.*, "Compositional and strain analysis of In(Ga)N/GaN short period superlattices," *J. Appl. Phys.*, vol. 123, no. 2, Jan. 2018, Art. no. 024304.

[14] K. Islam, M. Ploschner, and E. M. Goldys, "Multi-LED light source for hyperspectral imaging," *Opt. Exp.*, vol. 25, no. 26, pp. 32659–32668, Dec. 2017.

[15] M. Jones, C. H. Teng, Q. M. Yan, P. C. Ku, and E. Kioupakis, "Impact of carrier localization on recombination in InGaN quantum wells and the efficiency of nitride light-emitting diodes: Insights from theory and numerical simulations," *Appl. Phys. Lett.*, vol. 111, no. 11, Aug. 2017, Art. no. 113501.

[16] Y. Lin *et al.*, "Evolution of crystal imperfections during current-stress ageing tests of green InGaN light-emitting diodes," *Appl. Phys. Exp.*, vol. 9, no. 9, Aug. 2016, Art. no. 092101.

[17] Y. Lin *et al.*, "An introduction on microscopic-hyperspectral imaging for GaN-based LED investigation," *Proc. SPIE.*, vol. 10554, Feb. 2018, Art. no. 1055416.

[18] H. Jeong *et al.*, "Carrier localization in In-rich InGaN/GaN multiple quantum wells for green light-emitting diodes," *Sci. Rep.*, vol. 5, no. 9373, pp. 1–7, Mar. 2015.

[19] Y. Lin *et al.*, "Defects dynamics during ageing cycles of InGaN blue light-emitting diodes revealed by evolution of external quantum efficiency-current dependence," *Opt. Exp.*, vol. 23, no. 15, pp. 79–86, Jul. 2015.

[20] C. K. Li *et al.*, "Localization landscape theory of disorder in semiconductors. III. Application to carrier transport and recombination in light emitting diodes," *Phys. Rev. B*, vol. 95, no. 14, Apr. 2017, Art. no. 144206.

[21] T. J. Yang, R. Shivaraman, J. S. Speck, and Y. R. Wu, "The influence of random indium alloy fluctuations in indium gallium nitride quantum wells on the device behavior," *J. Appl. Phys.*, vol. 116, no. 11, Sep. 2014, Art. no. 113104.

[22] W. Liu *et al.*, "Localization effect in green light emitting InGaN/GaN multiple quantum wells with varying well thickness," *J. Alloys Compd.*, vol. 625, no. 15, pp. 266–270, Mar. 2015.

[23] W. Liu *et al.*, "Temperature dependence of photoluminescence spectra for green light emission from InGaN/GaN multiple wells," *Opt. Exp.*, vol. 23, no. 12, pp. 15935–15943, Jun. 2015.

[24] I. H. Lee *et al.*, "Point defects controlling non-radiative recombination in GaN blue light emitting diodes: Insights from radiation damage experiments," *J. Appl. Phys.*, vol. 122, no. 11, Sep. 2017, Art. no. 115704.

[25] Z. Li *et al.*, "Two distinct carrier localization in green light-emitting diodes with InGaN/GaN multiple quantum wells," *J. Appl. Phys.*, vol. 115, no. 8, Feb. 2014, Art. no. 083112.

[26] T. T. Chen, C. P. Wang, H. K. Fu, P. T. Chou, and S. P. Ying, "Electroluminescence enhancement in InGaN light-emitting diode during the electrical stressing process," *Opt. Exp.*, vol. 22, no. 5, pp. 1328–1333, Aug. 2014.

[27] Q. Wang, X. G. Gao, Y. L. Xu, and J. C. Leng, "Carrier localization in strong phase-separated InGaN/GaN multiple-quantum-well dual-wavelength LEDs," *J. Alloys Compd.*, vol. 726, no. 5, pp. 460–465, Dec. 2017.

[28] J. Yang *et al.*, "Performance enhanced by inserting an InGaN/GaN shallower-quantum well layer in InGaN based green laser diodes," *IEEE Photon. J.*, vol. 9, no. 2, Apr. 2017, Art. no. 2300108.

[29] J. Glaab *et al.*, "Degradation of (InAlGa)N-based UV-B light emitting diodes stressed by current and temperature," *J. Appl. Phys.*, vol. 118, no. 9, Sep. 2015, Art. no. 094504.

[30] D. H. Lee, B. Mitchell, Y. Fujiwara, and V. Dierolf, "Thermodynamics and kinetics of three Mg-H-V_N complexes in Mg:GaN from combined first-principles calculation and experiment," *Phys. Rev. Lett.*, vol. 112, no. 20, May 2014, Art. no. 205501.

[31] M. Meneghini, M. D. Lago, N. Trivellin, G. Meneghesso, and E. Zanoni, "Degradation mechanisms of high-power LEDs for lighting applications: An overview," *IEEE Trans. Ind. Appl.*, vol. 50, no. 1, pp. 78–85, Jun. 2014.

[32] N. Shmid *et al.*, "Peculiarities of defect generation under injection current in LEDs based on A^3N nanostructures," *Phys. Status Solidi C*, vol. 12, no. 8, pp. 1136–1139, May 2015.

[33] D. Monti, M. Meneghini, C. D. Santi, G. Meneghesso, and E, Zanoni, "Degradation of UV-A LEDs: Physical origin and dependence on stress conditions," *IEEE Trans. Device Mater. Rel.*, vol. 16, no. 2, pp. 213–219, Jun. 2016.

[34] S. Hafiz *et al.*, "Determination of carrier diffusion length in GaN," *J. Appl. Phys.*, vol. 117, no. 1, Jan. 2015, Art. no. 013106.

[35] A. Kaneta, M. Funato, and Y. Kawakami, "Nanoscopic recombination processes in InGaN/GaN quantum wells emitting violet, blue, and green spectra," *Phys. Rev. B*, vol. 78, no. 12, Sep. 2008, Art. no. 125317.